12-17-2004

In Vitro Metabolism Study of Brevetoxins by LC-ESI-MS

Weiqun Wang
University of New Orleans

IN VITRO METABOLISM STUDY OF BREVETOXINS BY LC-ESI-MS

A Thesis

Submitted to the Graduate Faculty of the
University of New Orleans
in the partial fulfillment of the
requirements for the degree of

Master of Sciences
in
The Department of Chemistry

by

Weiqun Wang

B.S. Nankai University, China, 1989

December, 2004

ACKNOWLEDGEMENT

I must extend my greatest gratitude and appreciation to the following people who have been supporting me all the time.

I would like to begin by thanking my advisor: Professor Richard B. Cole for all his guidance and advice. I am very grateful to him for spending time with me to answer all my questions in research and correct my thesis.

I would like to thank the committee members: Professor Zeev Rosenzweig, Professor Matthew A. Tarr, Professor Guangdi Wang and Professor Ronald F. Evilia for their valuable suggestions for the project. I would also like to particularly thank Dr. Guangdi Wang for generously providing the liquid-chromatograph instrument of his research group for this study, and to Mr. Qiang Zhang for his helpful advises for experiments.

I also want to take this opportunity to thank my colleagues: Bryan Ham, Bing Guan, Kan Chen, Chanel Fortier, Dr. Boguslaw Pozniac and former group members Dr. Yang Cai, Dr. Yan Li for their assistance during my graduate studies.

TABLE OF CONTENTS

LIST OF FIGURES

ABSTRACT

Brevetoxins are natural neurotoxins that are produced by “red tide” algae. In this study, brevetoxin-1 and brevetoxin-2 were incubated with rat liver hepatocytes and rat liver microsomes, respectively. After clean-up steps, samples were analyzed by liquid chromatography (LC) coupled with electrospray mass spectrometry (LC-MS). For the incubation sample of brevetoxin-1, two metabolites were found: brevetoxin-1-M1 and brevetoxin-1-M2. The tandem mass spectrometry study of the $[\text{brevetoxin-1-M1+H}]^+$ led to the conclusion that it was formed by converting one double bond in the E or F ring of brevetoxin-1 into a diol. The second metabolite (brevetoxin-1-M2) is proposed to be a hydrolysis product of brevetoxin-1 involving opening of the lactone ring with the addition of a water molecule. The study of incubation of brevetoxin-2 found two metabolites: brevetoxin-2-M1 gave a large $[\text{M-H}]^-$ peak, and its product ion mass spectrum allowed the deduction that this metabolite was the hydrolysis product of brevetoxin-2; the second metabolite (brevetoxin-2-M2) was deduced to have the same structure as that of brevetoxin-3.

CHAPTER I INTRODUCTION

Brevetoxins are natural toxins that are produced from a single cell dinoflagellate *Gymnodinium breve* that is responsible for blooms of “red tide” algae(1). This algae can grow rapidly under appropriate conditions of nitrate concentration, salinity, water depth and other factors(2). Outbreaks of “red tide” have been a recurring problem in the Gulf of Mexico in recent years. In fact, it is reported that since the 1970s, the rate of reoccurrence of this harmful algal bloom in the US has increased. For example, the *Gymnodinium breve* outbreak off the western coast of Florida occurs every 3-5 years (3). The toxins produced from such algae are lipid soluble polyether neutrotoxins that can cause massive fish kills. They also can cause human health hazards such as food (shellfish) poisoning(4), respiratory problems, eye irritation and skin irritation (5-7). Such harmful blooms usually impair the fishery industries (e.g. causing closing of shellfish beds), as well as the tourism industry. For example, in October of 1996, a *Gymnodinium Breve* bloom occurred in the shellfish harvesting waters (Gulf of Mexico) off of Louisiana, Mississippi and Alabama; brevetoxin-2 dominated the *Gymnodinium breve* toxin profile in the bloom. The shellfish toxicity exceeded the guidance level for 75 days even after the bloom had dissipated(8). Also in the spring of that same year, a bloom of *Gymnodinium breve* appeared along the southwest coast of Florida, and at least two hundred manatees were found dead or dying in the coastal waters, or on beaches, in an ecological disaster(9).

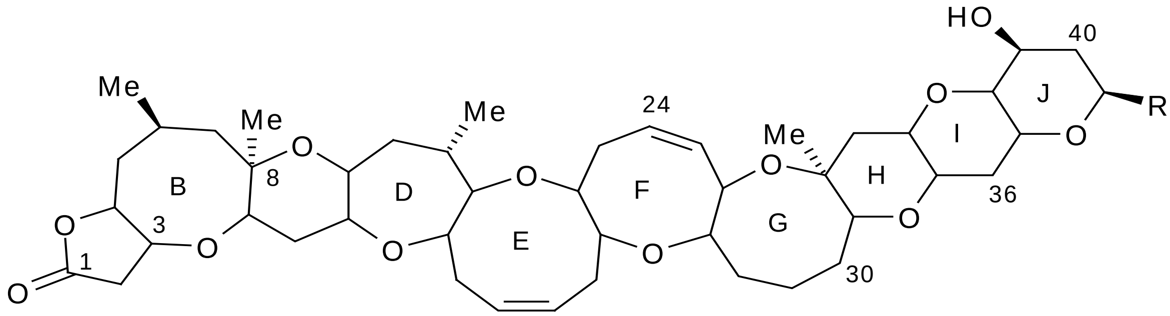

(monoisotopic mass, M_r)

Type-A Brevetoxins: Btx-1, R = $CH_2C(=CH_2)CHO$ (866.5)
Btx-7, R = $CH_2C(=CH_2)CH_2OH$ (868.6)
Btx-10, R = $CH_2CH(CH_3)CH_2OH$ (870.6)

For Btx-2, R =

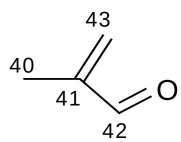

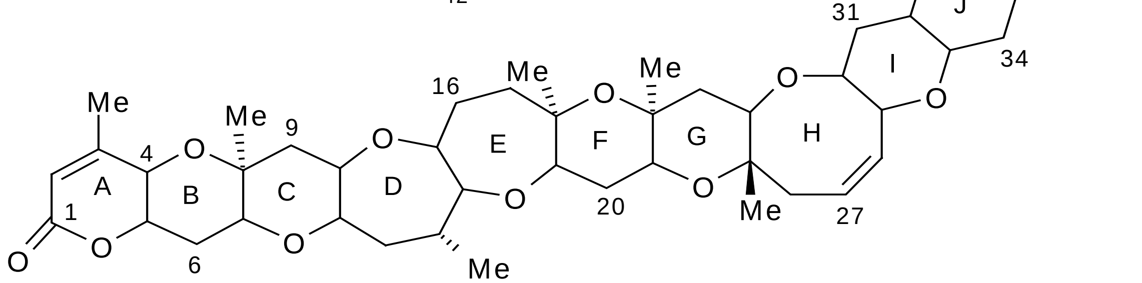

(monoisotopic mass, M_r)

Type-B Brevetoxins: Btx-2, R = $CH_2C(=CH_2)CHO$ (894.6)
Btx-3, R = $CH_2C(=CH_2)CH_2OH$ (896.6)
Btx-8, R = CH_2COCH_2Cl (916.4)
Btx-9, R = $CH_2CH(CH_3)CH_2OH$ (898.6)
Btx-5, the K-ring acetate of Btx-2 (936.6)
Btx-6, the H-ring epoxide of Btx-2 (910.6)

Figure 1. General structure of the two main types of brevetoxins

The structures of brevetoxins are complicated and their molecular weights are nearly 1000 Da, so the structural elucidation of these compounds is quite challenging. In 1981, Lin et al. (10) first reported the structural identification of brevetoxin-2, the most naturally abundant brevetoxin species. Since then, there are a total of nine brevetoxins that have been structurally elucidated(4, 11, 12). Based on their backbone structures, they can be divided into two categories (Figure 1): type A, which has 10 polyether rings; and type B, which has 11 polyether rings.

The physiological effects of brevetoxins are mainly neurotoxic symptoms in animals and humans. This type of toxin can induce central depression of respiratory and cardiac functions, spontaneous muscle contractions, spasms and rhinorrhea(13). The toxicity of brrevetoxins stems from the fact that they bind to a specific receptor site in the voltage sensitive sodium channel (VSSC) in the cell membrane(4). Binding involves a complicated series of association-dissociation events, and the whole binding process may need several hours to reach equilibrium (14). It is hypothesized that the binding of brevetoxins to this VSSC receptor site will push the channel in favor of its open conformation, thus shifting the channel activation voltage and prolonging the activation duration time, while inhibiting its inactivation function(15). Over time, cells can no longer conduct their functions properly, and many symptoms such as hypertension and arrhythmia will occur. In clinical animal trials, the symptoms could lead to death(13).

Currently, there are only a few reports on metabolite studies of brevetoxins, and these mainly pertain to metabolites found in shellfish. A case study of shellfish poisoning in Florida

found four major metabolites by HPLC-MS and radioimmunoassy(16). One is identified as brevetoxin-3, which was likely produced by reduction of the dominant parent toxin brevetoxin-2. When detected in the form of protonated molecules, $[M+H]^+$, the remaining three metabolites appear at m/z 1018, 1034 and 1005, however, their structures were not determined. In 1993, more than 280 people suffered from shellfish poisoning in New Zealand in a single incident (17, 18) related to consumption of “Greenshell Mussels”. Two major metabolites were separated and identified: One appeared at m/z 1135.7 in negative mode FAB-MS. Combined with information obtained from NMR studies, the structure was determined to be a D-ring opening of brevetoxin-2 with esterification of the resulting alcohol and oxidation of the terminal aldehyde oxidized to the acid form (17),(19). The other metabolite appeared at m/z 1034.5 in its protonated form. It can be described as a 1,4-addition of L-cysteine to the terminal side chain group of brevetoxin-2 followed by oxidation of the sulfide to sulfoxide and reduction of the aldehyde to an alcohol(18). However, studies on the metabolic pathways of brevetoxins in mammalian species are still rare. An early study in 1989 reported the observation of two metabolic products in rat liver hepatocytes using a radiolabeled compound. However, the structures of these two metabolites were not elucidated(20).

In the current study, rat liver microsomes were applied to the *in vitro* metabolism study of brevetoxin-2, the dominant species of brevetoxins, and high performance liquid chromatography coupled with tandem mass spectrometry was used for separation and identification of metabolic products. On the other hand, brevetoxin-1 was incubated with rat hepatocytes and analyzed by similar LC-MS/MS approaches.

Because liver is the major organ for toxic chemical biotransformation, it is the tissue of choice for metabolism and toxicity studies. The metabolite profile of a drug obtained *in vitro* generally reflects the *in vivo* metabolite pattern, although limited to qualitative aspects(21). Because of this, *in vitro* metabolism techniques involving liver tissue including isolated liver hepatocytes and microsomes have been developed(22). Liver microsomes are prepared by homogenization of liver(s), followed by centrifugation of the homogenate at 9,000 to 10,000 times the force of gravity to yield a supernatant subcellular fraction (also known as S9 or S10) (23). Microsomes contain many xenobiotic-metabolizing enzymes, the most prominent group of enzymes is the family of cytochrome P450 (CYPs). These enzymes play a key role in the metabolism of a variety of chemically diverse compounds.

Like liver microsomes, hepatocytes are also widely employed in *in vitro* metabolism studies. Hepatocytes are isolated from liver by so-called two-step collagenase digestion procedures. A freshly isolated liver is perfused first with an isotonic buffer solution containing a calcium chelating agent to clear the blood and to loosen cell-cell junctions, followed by a collagenase solution to dissociate the hepatocytes from the liver parenchyma(24). Cryopreserved hepatocytes are also available, but some enzyme reactivity (including P450) might be lower than that of freshly isolated hepatocytes. Due to this, and the commercial shortage of fresh liver, many laboratories favor liver microsomes since they can be prepared and purchased in large batches and preserved at –80 °C for many months with little loss of P450 activity(25).

CHAPTER II EXPERIMENTAL

2.1 Materials

Brevetoxin-1 was purchased from Chiral Corp. (Miami, FL), Brevetoxin-2 and brevetoxin-3 were purchased from CalBiochem (La Jolla, CA), HPLC-grade methanol and water were purchased from EM Sciences (Gibbstown, NJ). Rat hepatocyte wells were purchased from CEDRA Corp. (Austin, TX); rat liver microsomes and NADPH regenerated system were purchased from Genetest Corp. (Woburn, MA).

2.2 **Microsomal incubation**

According to the basic approach of Degawa et al (26), 2 μL of 5 mM brevetoxin-2 in ethanol was added to the incubation system as the substrate, the incubation mixture also included rat liver microsomes (at 1.5 mg/mL protein concentration), 16.5 mM glucose-6-phosphate, 16.5 mM magnesium chloride, and 70 mM potassium phosphate buffer (pH 7.4) to make 0.1 mL aliquots each containing 0.1 mM brevetoxin-2(27). The incubation was conducted in a VWR 1225 (Cornelius, OR) water bath at 37 °C for 12-24 hours. Blank and control incubations were also conducted, including incubation in the absence of microsomes, incubation in the absence of brevetoxin-2, and incubation in the absence of NADPH regenerating system. The incubation was

stopped by adding an equal volume of ice cold methanol; the mixture was then vortexed and centrifuged, and the supernatant was passed through a microcon YM-3 filter (Pittsburgh, PA) to further remove protein.

2.3 Rat hepatocytes incubation

The procedure was based on the method of Ekwall et al(28). Substrate solution (10 μg brevetoxin-1 in 1 mL William E medium) was added into a rat hepatocyte well containing about 1 million cells. After 24 hours incubation at 37 ^{0}C in a 5% CO_2 incubator, the incubation was stopped by adding 2 mL CH_3CN. The solution was filtered (0.2 μm) and evaporated to 0.8 mL to eliminate virtually all organic solvent(29). Blank and control tests were also performed; for the controls, brevetoxin-1 was added after the incubation was quenched. The solution containing substrate and metabolites was cleaned up by solid phase extraction and concentrated to 100 μL prior to LC/MS analysis.

2.4 LC-MS and LC-MS/MS Analysis

After incubation and protein clean-up, the brevetoxin-2 incubation sample was separated by liquid chromatography (LC) equipped with parallel LC-10 ADVP pumps and UV-Vis SPD-10ADVP detector (Shimadzu Instruments Co. Colombia, MD). A 2.1 x 100 mm, 3.5 μm C-18 Agilent (Wilmington, DE) LC column, coupled with 2.1 x 12.5 mm Agilent (Wilmington, DE) C-18 guard column was employed to separate the mixture. The mobile phase was 80:20 methanol:water for the first 2.5 minutes, then linearly changed to 90:10 methanol:water in one minute. The flow rate was set at 0.2 mL/min. The brevetoxin-1 sample was separated on a 1 x 100 mm, 3 μm C-18 Spherisorb column (ISCO, Lincoln, NE), with an isocratic mobile phase (85:15 methanol/water at 20 μL/min). After exiting the column, the LC eluents were directly infused into the Quatro II triple-quadrupole mass spectrometer, equipped with an electrospray ionization source (Micromass Inc. Manchester, UK). Nitrogen gas was employed as both drying gas and nebulizing gas. The ES "needle" voltage was set at 3.7 kV, and the cone voltage was set at 40 V, for both positive and negative modes. Collision-induced decomposition (CID) tandem mass spectra were acquired at 70-75 eV collision energy, using argon as collision gas at a pressure of 2.1×10^{-4} mbar (gauge external to cell). All mass spectra represent the average of 10 to 20 scans. To make accordance with the nitrogen rule, all reported m/z values were rounded down to the nearest integer values. Therefore, because there is no nitrogen atom in brevetoxin and its metabolites, all brevetoxin molecules and their fragments should be even-electron, and the corresponding peaks in electrospray mass spectra should appear only at odd mass values.

CHAPTER III RESULTS AND DISCUSSION

3.1 Brevetoxin-2 metabolism

The brevetoxin-2 sample subjected to incubation with rat microsomes will be examined first. The LC-MS traces obtained after injection of the filtered incubation sample are shown in Figure 2. Two main metabolite peaks were observed in addition to the peak representing unreacted brevetoxin-2. The averaged mass spectrum for the first chromatographic peak at 4.3 min (Figure 2b), representing the metabolite that we are calling brevetoxin-2-M1, showed mass spectral peaks at both m/z 935 and 951 (Figure 3a), which suggested that these could be the sodium and potassium adducts, respectively, of a neutral molecule of 912 Da. The averaged mass spectrum for the second chromatographic peak at 7.8 min (Figure 2c), which represents the second metabolite that we are calling brevetoxin-2-M2, showed m/z 919 as the base peak and also m/z 935 (Figure 3b). The third peak on the chromatogram at 8.5 min (Figure 2d) also showed two peaks, i.e., m/z 917 as base peak and m/z 933 (Figure 3c), which represent the sodium and potassium adducts of unreacted brevetoxin-2 in the incubation solution. Selected ion chromatograms of m/z 917 (Figure 2d) and 919 (Figure 2c), clearly show the peaks for sodium adducts of brevetoxin-2 and its metabolite, respectively. No other significant peak was found by searching selected ion chromatograms of other m/z values, nor by extending the chromatographic running time. Based on this information, we postulate that the second chromatographic peak at 7.8 min corresponds to the sodium and potassium adducts

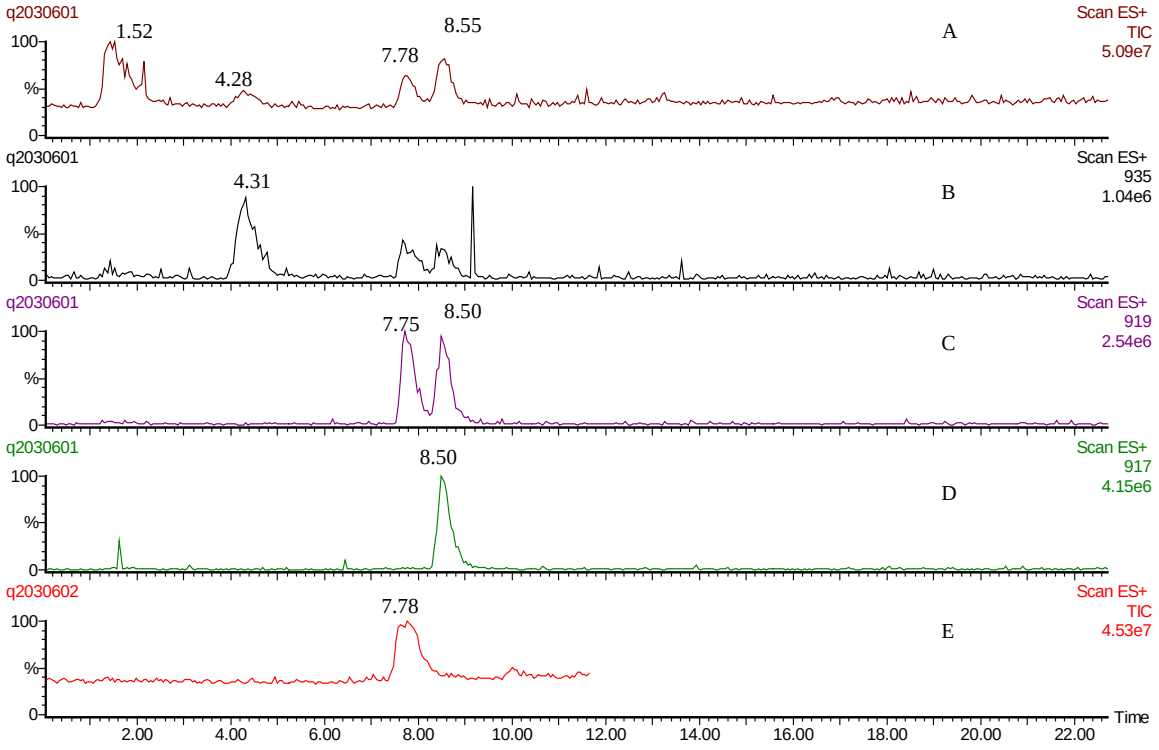

Figure 2. LC-MS chromatograms for brevetoxin-2 rat microsomes incubation sample and a brevetoxin-3 standard. a) TIC for incubation sample. b) SIC of m/z 935 from the incubation sample. The peak at 4.31 min represents metabolite brevetoxin-2-M1. $[M+Na]^+$ of unreacted brevetoxin-2, from the incubation sample; c) SIC of m/z 919 from the incubation sample. In this chromatogram, the peak at 7.75 min represents a metabolite brevetoxin-2-M2, whereas the peak at 8.50 min is the M+2 peak of unreacted brevetoxin-2. d) SIC of m/z 917, $[Brevetoxin\text{-}2+Na]^+$, of unreacted substrate from the incubation sample. 2e) TIC for brevetoxin-3 standard. The retention time of brevetoxin-3 overlaps that of brevetoxin-2-M2.

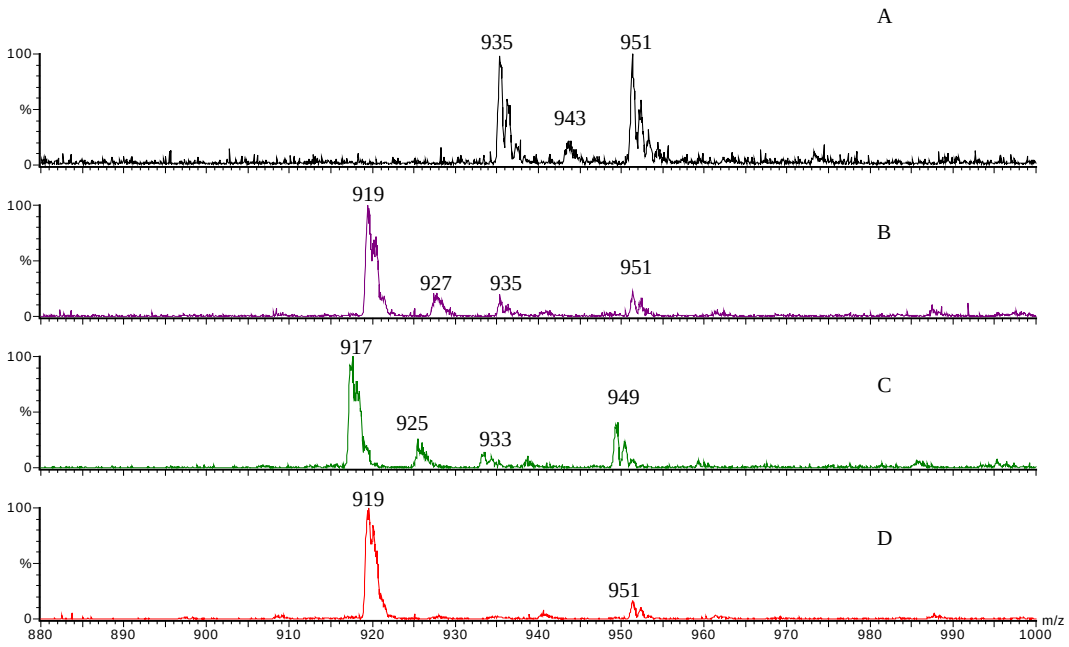

Figure 3. Mass spectra corresponding to major peaks observed in Figure 2. a) The peak at 4.3 min is assigned as Brevetoxin-2-M1, the hydrolysis product of brevetoxin-2. m/z 935 and 951 correspond to sodium and potassium adducts, respectively; m/z 943 represents [brevetoxin-2-M1+Na+K]$^{2+}$. b) The peak at 7.8 min is assigned as Brevetoxin-2-M2, a reduced form of brevetoxin-2, i.e., brevetoxin-3: m/z 919 represents [brevetoxin-2-M2+Na]$^{+}$, m/z 935 is [brevetoxin-2-M2+K]$^{+}$, m/z 927 is the doubly charged dimer of the above two species, and m/z 951 is [brevetoxin-2-M2+Na+MeOH]$^{+}$. c) The peak at 8.5 min corresponds to unreacted brevetoxin-2: m/z 917 represents [brevetoxin-2+Na]$^{+}$, m/z 933 is [brevetoxin-2+K]$^{+}$, m/z 925 is the doubly charged dimer of the above two species, and m/z 949 is [brevetoxin-2+Na+MeOH]$^{+}$. Note that each peak is shifted toward lower m/z by two units as compared to 3b. d) Brevetoxin-3 standard. m/z 919 is the sodium adduct of brevetoxin-3, and m/z 951 is the sodium-plus-methanol adduct of brevetoxin-3.

of the metabolite brevetoxin-2-M2 of mass 896 Da, which has the same molecular weight as brevetoxin-3 (see Figure 1).

We postulate that brevetxin-2-M2 is formed by metabolic reduction of the tail (addition of two hydrogen atoms to the aldehyde), thereby forming brevetoxin-3. To confirm the postulation that the peak at 7.8 min (brevetoxin-2-M2, Figure 2) has the same structure as brevetoxin-3, LC-MS of a brevetoxin-3 standard in methanol (0.05 mM) was conducted, and its retention time (7.78 min figure 2e was found to be the same as that of brevetoxin-2-M2 under the same chromatographic conditions. The averaged mass spectrum of this standard (Figure 3d) also gave a signal at m/z 919, but did not give a strong signal at m/z 935 (no potassium adduct). This could be rationalized by considering that the brevetoxin-3 standard (with ubiquitous sodium contamination) was dissolved in pure methanol, whereas the incubation sample is actually in a solution of potassium phosphate buffer (pH 7.4). Brevetoxins have very strong binding affinities for sodium ion, and even trace levels of sodium in the system are already enough for brevetoxins to form sodium adducts(30). Notably, peaks corresponding to noncovalent methanol addition to sodium adducts of brevetoxins were observed at m/z 951 in figure 3d, and at m/z 949 in figure 3c. Of course, these peaks appeared with the same retention times as the corresponding sodiated brevetoxin species. Lastly, doubly charged mixed adducts of brevetoxins containing Na^+ and K^+ were observed at m/z 943 in figure 3a, m/z 927 in figure 3b, and at m/z 925 in figure 3c(31).

To further confirm the postulation that the second metabolite peak was brevetoxin-3, tandem mass spectrometry was performed. However, CID of the sodium adduct of brevetoxins only yields Na^+, and no informative fragments(30). In order to obtain a more useful tandem mass

spectrum, protonated brevetoxin is a preferable precursor ion. In our study, both passing incubation mixture through the ionic exchange resin (Dowex 50WX8) and direct acidification with 0.4 M TFA were attempted to promote formation of protonated molecules; direct acidification yielded stronger signals, but the signal-to-noise ratios for protonated precursor molecules eluting during LC-MS were still not strong enough to obtain adequate product ion mass spectra. During the separation, apparently traces of sodium on the LC column and elsewhere converted protonated molecules back to sodium adducts. The approach of separating the incubation sample constituents with an acidic (TFA) mobile phase was also tried, but such conditions usually resulted in a raised chemical noise background that masked the $[M+H]^+$ signals.

The first metabolite peak (represented as brevetoxin-2-M1) has a deduced molecular weight of 912 Da, 18 Da higher than the mass of brevetoxin-2. We propose that this metabolite is a hydrolyzed form of brevetoxin-2. In negative mode LC-ES-MS operation, the incubation sample showed a large chromatographic peak at 4.2 min (Figure 4 inset). The negative ion mass spectrum corresponding to this peak, shown in figure 4, reveals the $[M-H]^-$ counterpart, at m/z 911, to the $[M+Na]^+$ ion (m/z 935) already seen in figure 2b and 3a. The fact that the intensity of m/z 911 was so much higher than any of the brevetoxins and brevetoxin metabolites in the negative ion mode suggests that this metabolite is likely to be a carboxylic acid. In fact, neither brevetoxin-2 nor brevetoxin-3 in pure solvent gives a significant signal in negative mode ES-MS. The problem is largely that the most acidic hydrogen atoms on brevetoxin-2 and brevetoxin-3 are the hydroxyl hydrogen atoms that are apparently not readily deprotonated under the employed

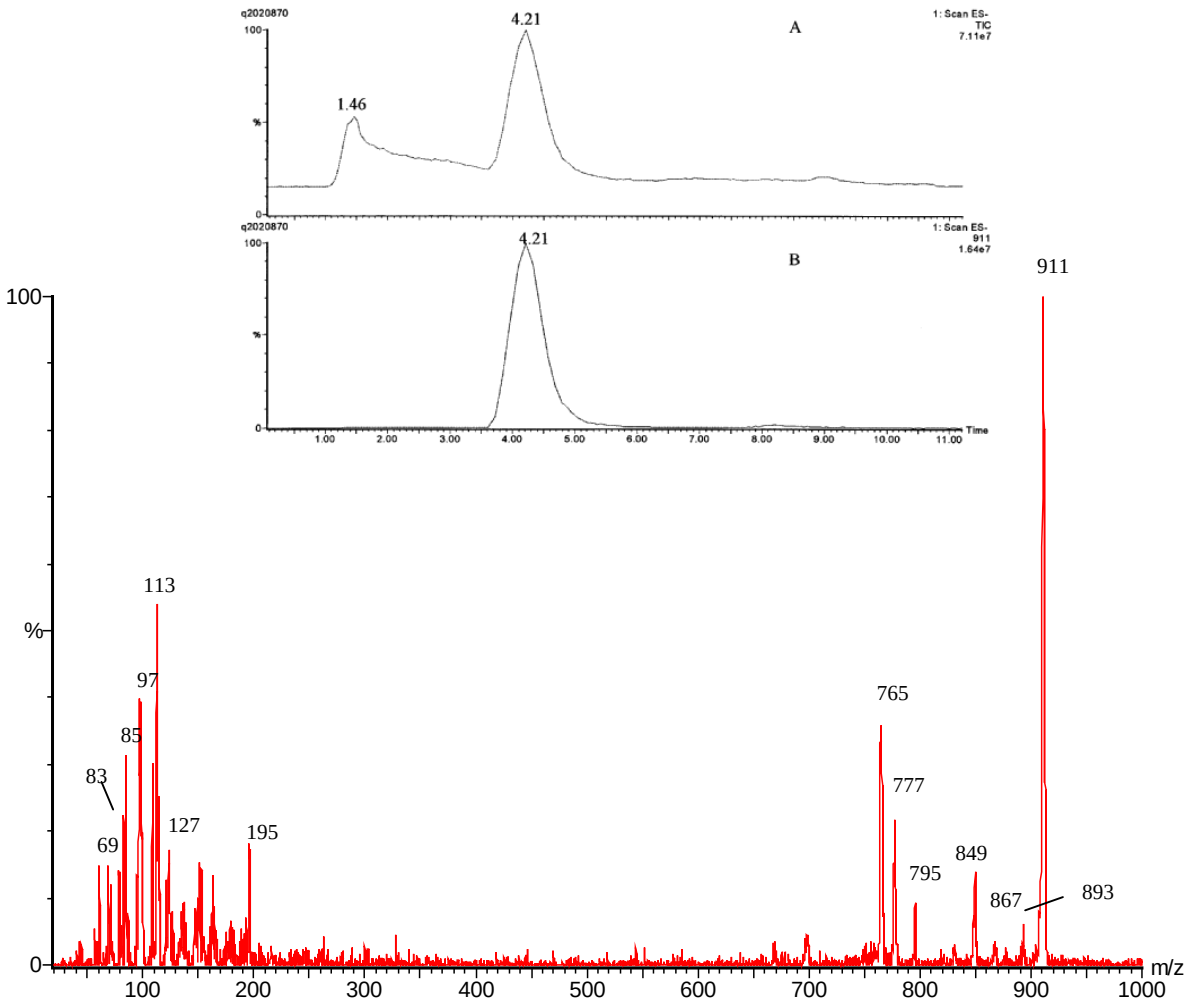

Figure 4: LC-MS/MS product ion mass spectrum of m/z 911, [brevetoxin-2-M1 - H]$^-$. (inset figure, LC-MS negative ion mode chromatograms for brevetoxin-2 incubation sample. a) TIC; b) SIC for m/z 911, the deprotonated form of the metabolite Brevetoxin-2-M1.

negative ion electrospray conditions. Tandem mass spectrometry of m/z 911 (figure 4) provided further evidence to support our proposed structure.

Figure 4 shows the LC-ES-MS/MS product ion spectrum of the m/z 911 precursor ion representing the deprotonated metabolite brevetoxin-2-M1. A charge remote fragmentation mechanism (Figure 5) can explain the formation of m/z 893 (by water loss), and subsequent charge induced CO_2 loss leads to m/z 849. Alternatively, CO_2 loss may occur first (yielding m/z 867, figure 6) with water loss occurring afterwards to form m/z 849. The latter m/z 849 ion can undergo charge remote loss of a 54 Da neutral to form m/z 795 (Figure 5), with subsequent water loss to produce m/z 777 (Figure 5). At a CID energy of 75eV (E_{LAB}), the hydrogen of the hydroxyl group on the B-ring may be transferred to the nearby carboxylic group (Figure 6 middle panel), thereby initiating two possible fragmentation pathways leading to fragments at m/z 113, the largest fragment peak in the figure 4 product ion spectrum, and m/z 69 (Figure 6). This same initial higher energy alkoxide form of m/z 911 is proposed to be responsible for the formation of m/z 85 (Figure 7), and m/z 127 (Figure 7). The latter can undergo CO_2 loss to form m/z 83 (Figure 7). The brevetoxin-2-M1 metabolite is apparently formed by opening of the head lactone ring with concomitant addition of a water molecule. This type of reaction can be accelerated by enzymes such as esterase or lactonase in the microsomes (32), (33). The proposed structures of brevetoxin-2-M1 and brevetoxin-2-M2 are shown in figure 8.

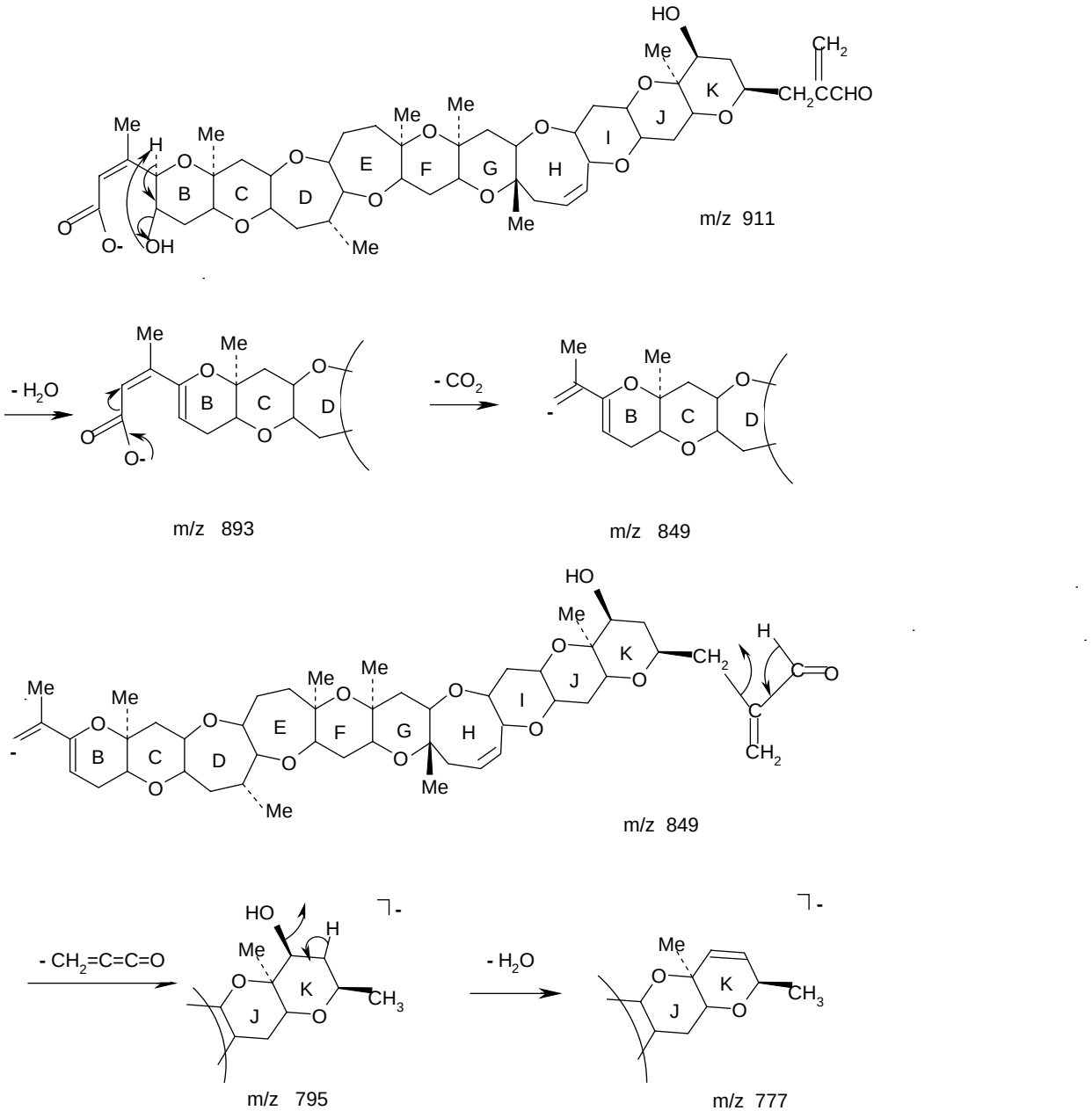

Figure 5. Proposed fragmentation of [brevetoxin-2-M1 - H]$^-$ (m/z 911), leading to formation of m/z 893, 849, 795 and 777.

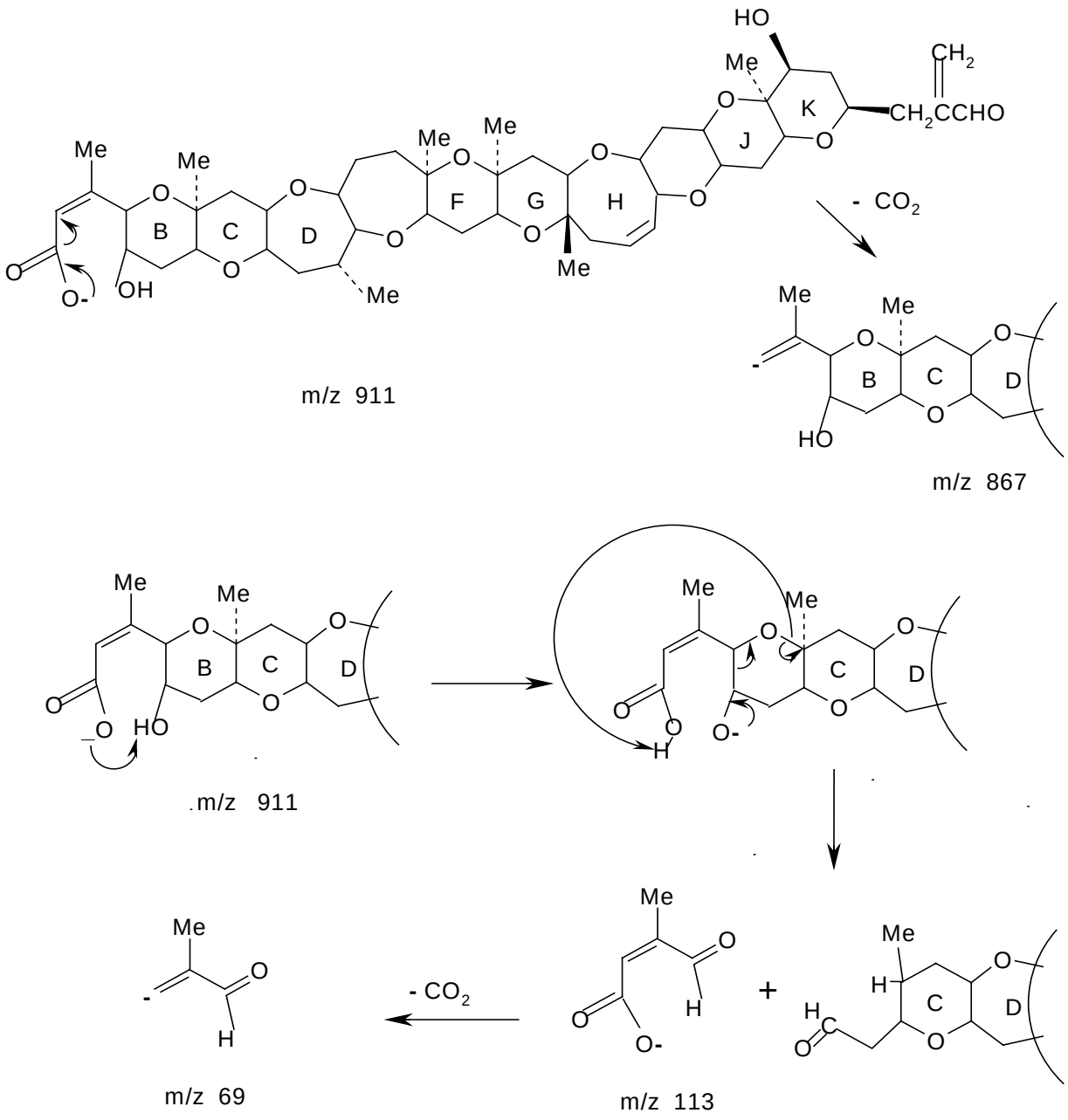

Figure 6. Proposed fragmentation mechanisms of [brevetoxin-2-M1 - H]$^-$ (m/z 911), leading to formation of m/z 867, 113 and 69.

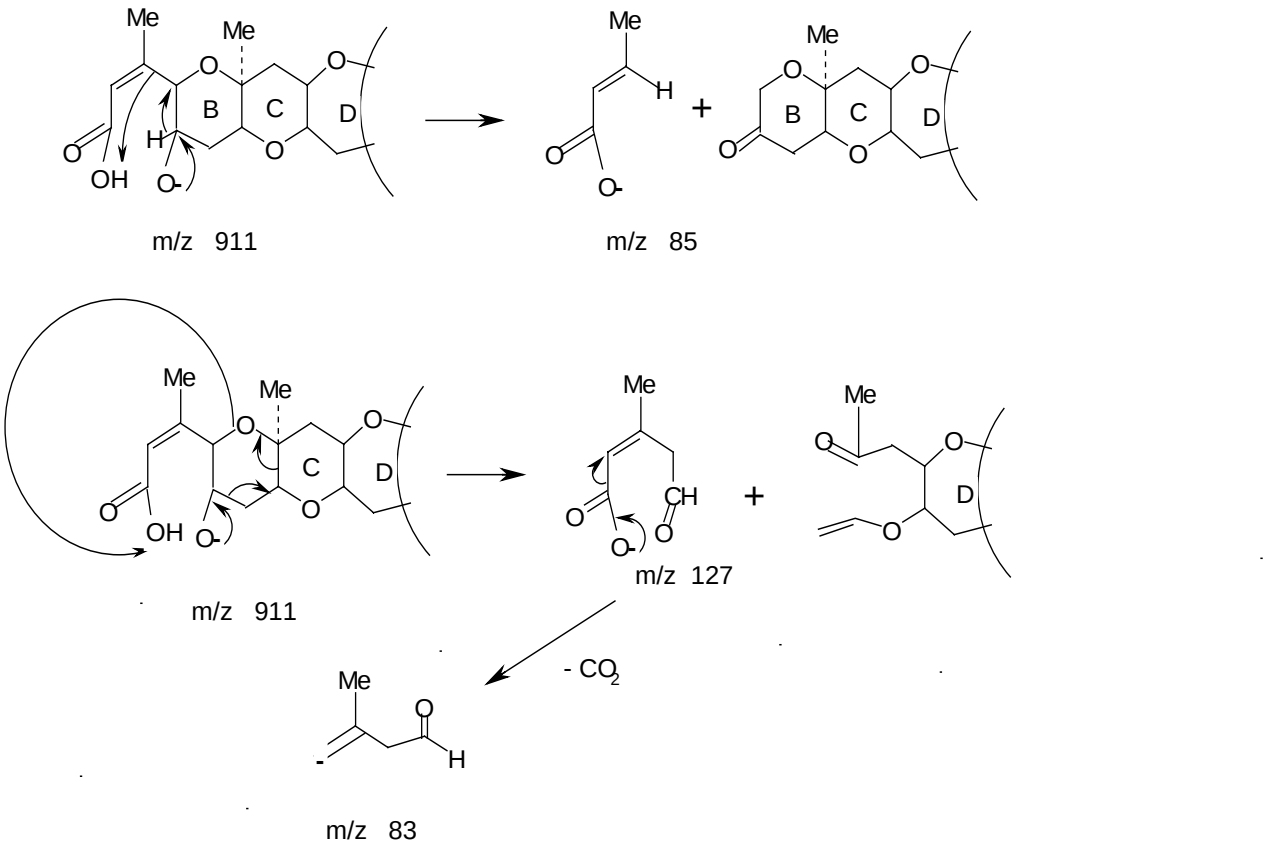

Figure 7. Proposed fragmentation mechanisms of [brevetoxin-2-M1 - H]$^-$ (m/z 911), leading to formation of m/z 85, 127 and 83

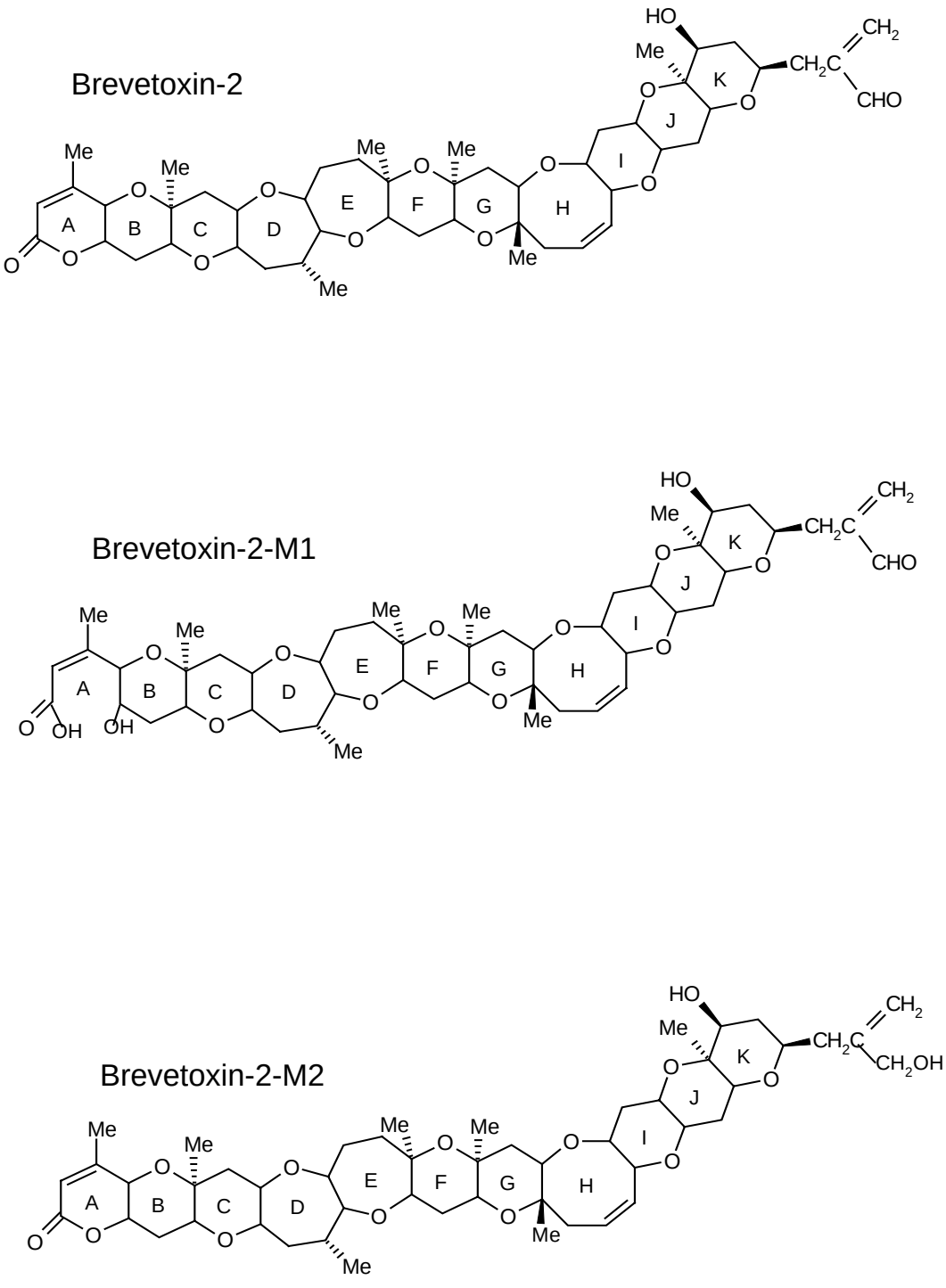

Figure 8. Proposed structures for the metabolites of brevetoxin-2

3.2 Brevetoxin-1 metabolism

After incubation of brevetoxin-1 with rat hepatocytes and clean-up, similar LC/MS approaches as above were applied to the analysis of the incubation samples. By searching the entire range of masses contained in the total ion chromatogram, three ion peaks were revealed, and their single ion chromatograms are shown in figure 9 peak retention times of 7.5 min, 8.0 min and 9.8 min in figure 9a, 9b, 9c, respectively. The peak retention time of 9.8 min in figure 9c and corresponding m/z value (889) are the same as those of the brevetoxin-1 standard starting material. This peak is clearly the sodium adduct [brevetoxin-1 + Na]$^+$ of the remaining substrate. The peaks in figure 9a (assigned as [brevetoxin-1-M1+Na]$^+$) and in figure 9b (assigned as [brevetoxin-1-M2 + Na]$^+$) are proposed to be the sodiated forms of two brevetoxin-1 metabolites. To verify the mass assignment of the sodiated ion, the same solution was acidified by HCl addition (1:1 ratio of sample:0.33 M HCl), and the resultant solution was injected into the LC/MS system. The obtained selected ion chromatograms did show peaks corresponding to the mass of protonated species that appeared at the same time as the sodiated ions. The peak in figure 10b was assigned as [brevetoxin-1-M1 + H]$^+$, and the peak in Figure 10d was assigned as [brevetoxin-1-M2 + H]$^+$. The polarity of these two brevetoxin metabolites appears to be greater than that of precursor brevetoxin-1, as the latter eluted later from the reversed phase C-18 column.

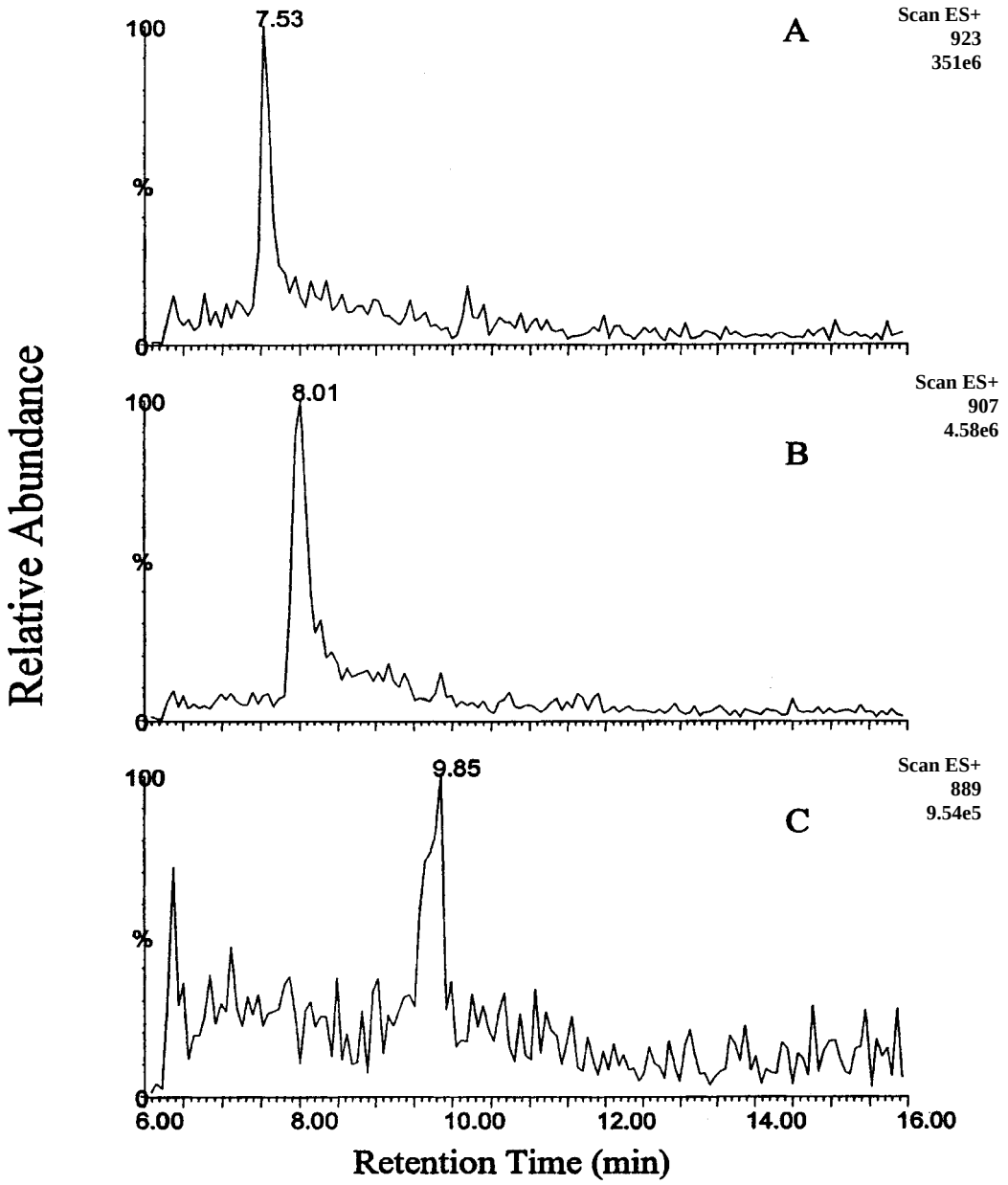

Figure 9. LC/MS selected ion chromatograms of brevetoxin-1 rat hepatocytes incubation sample. a) SIC of m/z 923, [Brevetoxin-1-M1 + Na]$^+$. b) SIC of m/z 907, [Brevetoxin-1-M2 + Na]$^+$. c) SIC of m/z 889, [Brevetoxin-1 + Na]$^+$.

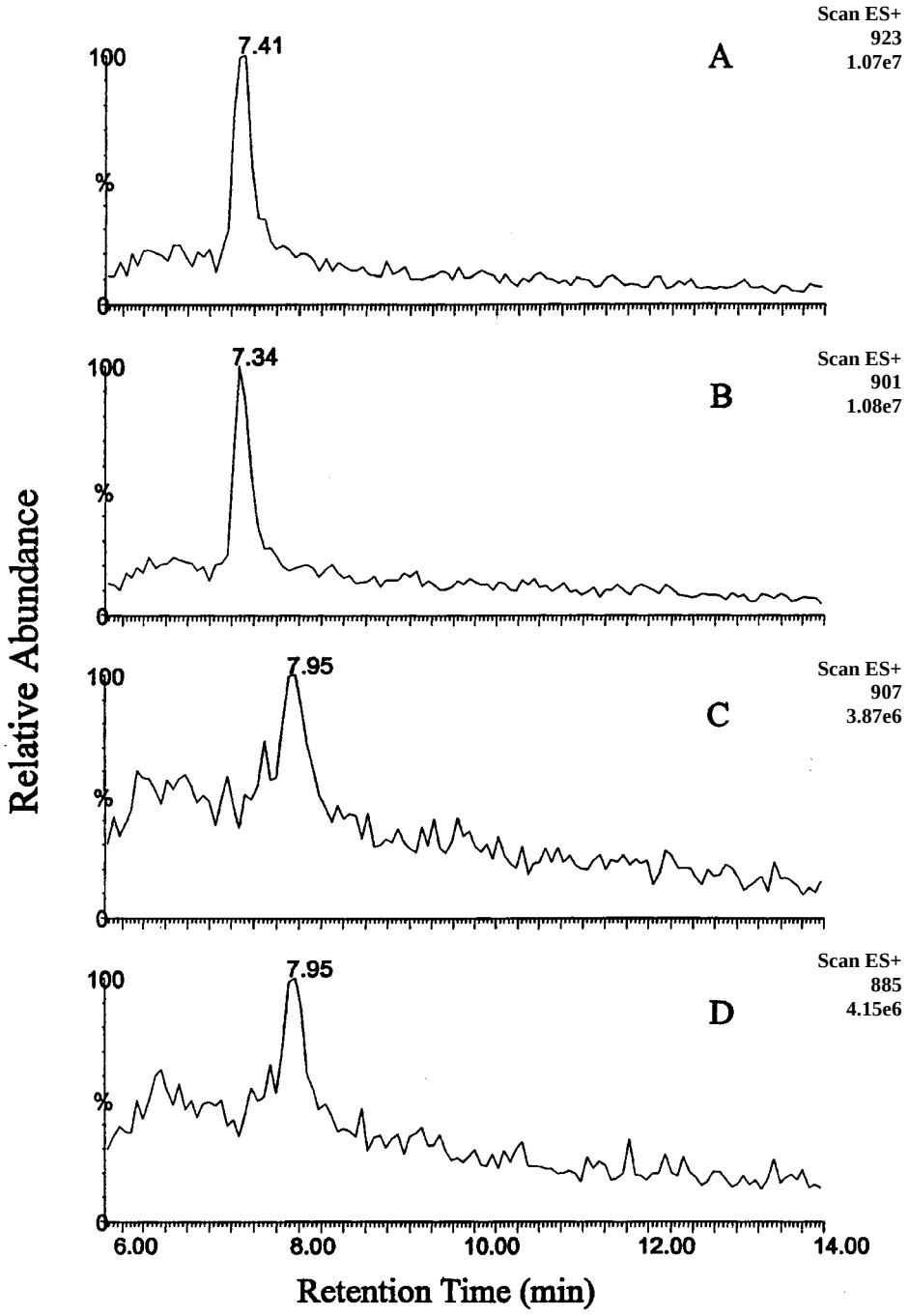

Figure 10. To examine the structures of metabolites, sample was acidified by 0.33 N HCl in a 1:1 ratio. The resultant solution showed peaks corresponding to protonated species that coexist with the sodiated ions in LC-MS. a). SIC for m/z 923, the peak of [Brevetoxin-1-M1+Na]$^+$. b) SIC for m/z 901, the peak of [Brevetoxin-1-M1+H]$^+$. c) SIC peak of [Brevetoxin-1-M2+Na]$^+$, m/z 907. d) SIC for m/z 885, [Brevetoxin-1-M2+H]$^+$.

To gain more insight into the structure of brvetoxin-1-M1, the product ion tandem mass spectrum of the [brevetoxin-1-M1 + H]$^+$ precursor was acquired and is shown in figure 12a. For comparison purposes, the product ion spectrum of the standard precursor [brevetoxin-1+H]$^+$ obtained under identical instrumental conditions is given in figure 12b. While at least three consecutive water losses are detectable from [brevetoxin-1-M1 + H]$^+$ (giving product ions at m/z 849, 831 and 813 in figure 12b), the water losses are much more prominent relative to other fragmentations for [brevetoxin-1-M1 + H]$^+$. In fact, the peak corresponding to loss of two water molecules (m/z 865) is even larger than the peak corresponding to a single water loss (m/z 883). Moreover, loss of a third water molecule (yielding m/z 847) gives a moderate signal relative to other product ions. The increased prominence of the second and third consecutive water losses for [brevetoxin-1-M1+H]$^+$ combined with its higher mass (34 Da) relative to brevetoxin-1 leads us to propose that brevetoxin-1-M1 is an oxidation product resulting from the metabolic conversion of a double bond on brevetoxin-1 into a diol. The question becomes: which of the three double bonds is converted to the diol?

In the lower ends of the product ion mass spectra, both figure 12a and 12b show peaks at m/z 55, 81 and 95, these peaks are proposed to be characteristic of the brevetoxin-1 side chain (Figure 13). Because these same peaks appear for decomposition of brevetoxin-1 and brevetoxin-1-M1, with no new peaks found for brevetoxin-1-M1 at m/z 89, 115 or 129, i.e. 34 Da higher than the proposed “tail” fragments for brevetoxin-1, it seems unlikely that the “tail” side chain unsaturation on brevetoxin-1-M1 is the site of diol conversion. Rather, we propose that diol formation is occurring on one of the two double bonds on the E or F ring (structures shown in Figure 11). The mechanism could be described as a two-step reaction wherein the double bond is

Brevetoxin-1

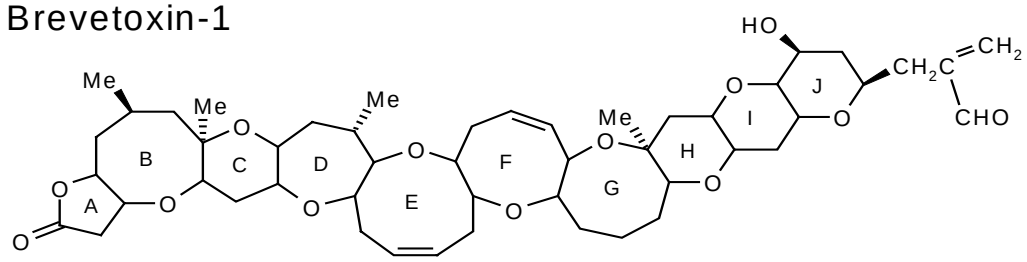

Brevetoxin-1-M1a

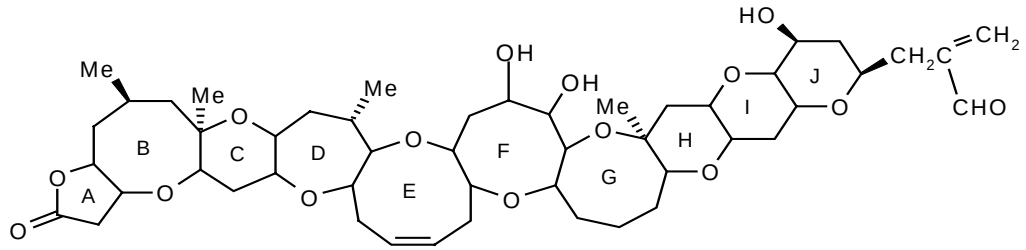

Brevetoxin-1-M1b

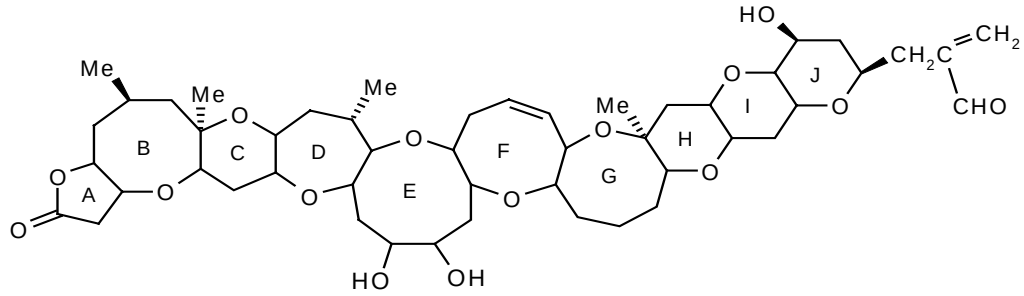

Brevetoxin-1-M2

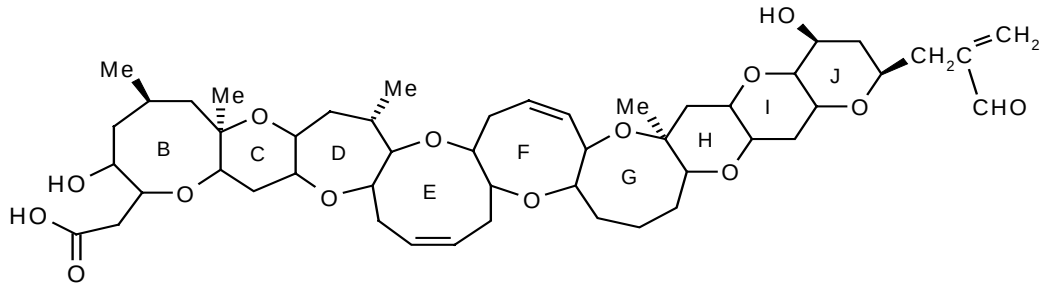

Figure11. Proposed structures for the metabolites of brevetoxin-1.

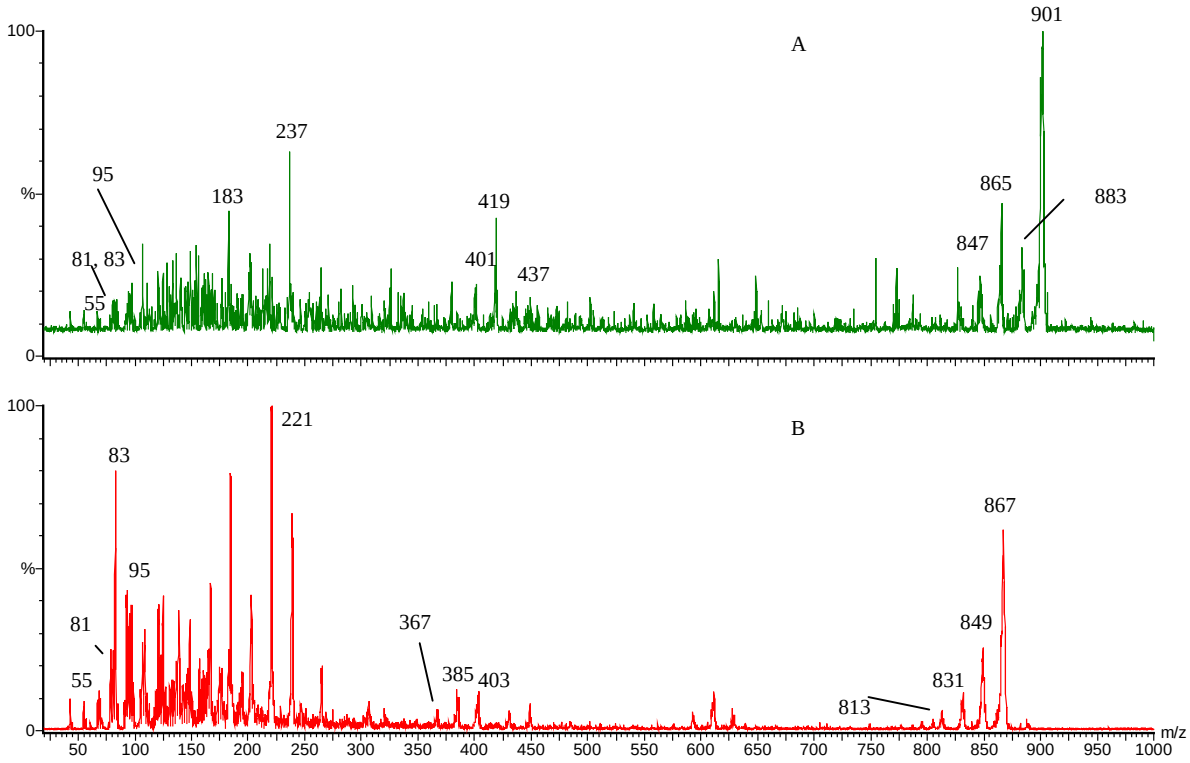

Figure 12. LC-MS/MS product ion mass spectra. a) m/z 901, protonated brevetoxin-1-M1 from incubation sample. b) m/z 867, $[\text{brevetoxin-1+H}]^+$ standard.

oxidized to form an epoxide structure catalyzed by enzyme P-450, followed by hydrolysis to form two hydroxyl groups. Further evidence to support the notion that a double bond on the E or F ring is converted to a diol is given by a comparison of the peaks at m/z 401, 419 and 437 in figure 12a which are 34 Da higher than those of m/z 367, 385 and 403 in figure 12b. This mass difference is the same as that shown by their precursor ions, which suggests that they may be formed by the same fragmentation pathways. The structure of the second metabolite, i.e., brevetoxin-1-M2, is proposed and shown in Figure 11. This metabolite is formed by opening of the lactone ring and by the addition of a water molecule. This kind of reaction can proceed spontaneously in aqueous solution and can be accelerated by enzymes such as esterase in the hepatocytes(34). The reaction is very much analogous to that involved in brevetoxin-2-M1 formation from brevetoxin-2 except that there, an unsaturated six-membered ring lactone was involved; whereas for brevetoxin-1, saturated five-membered ring undergoes hydrolysis (see figure 1).

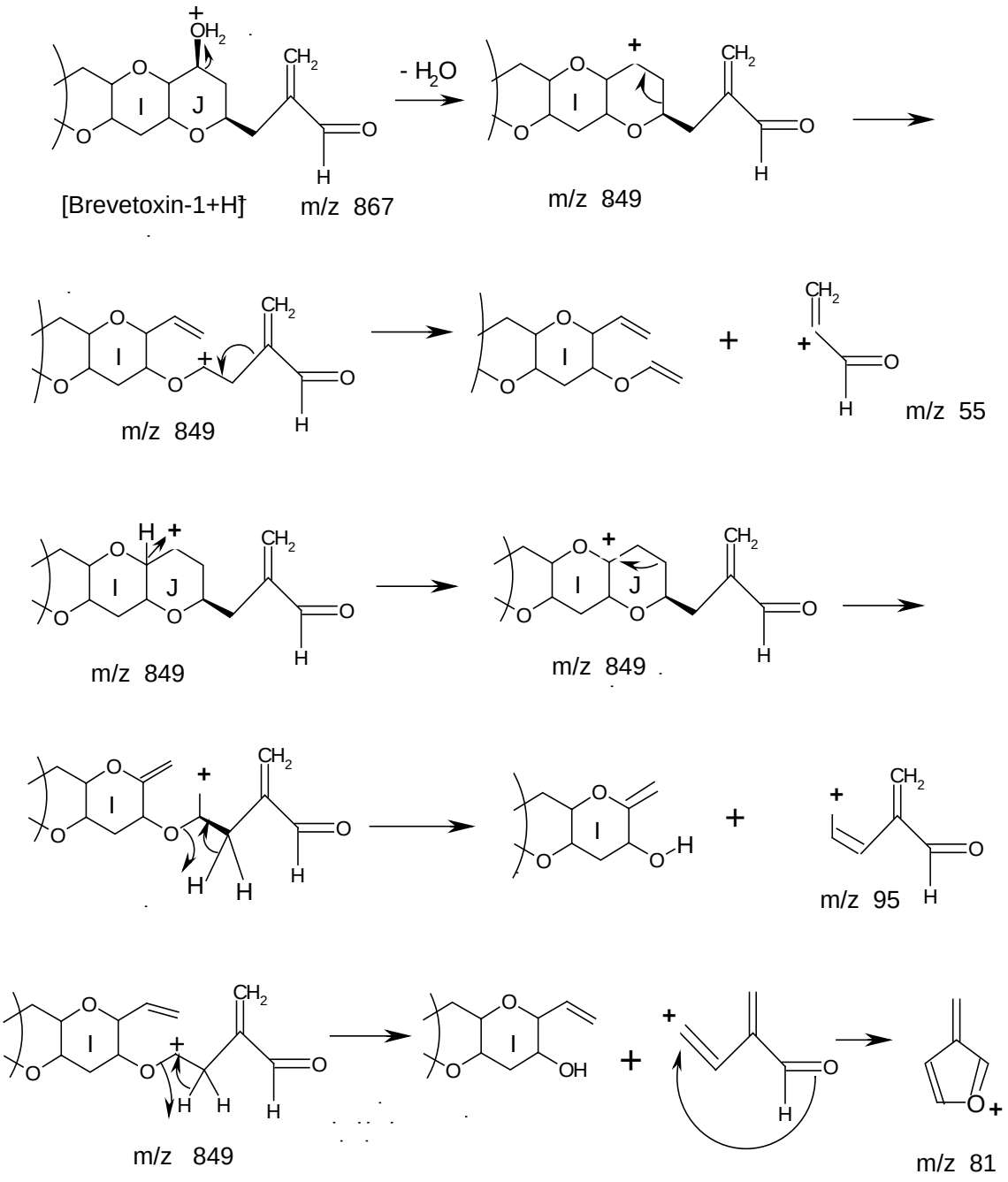

Figure 13. Proposed fragmentation mechanisms for “tail” portion side chain of [brevetoxin-1+H]$^+$ (m/z 867) leading to formation of m/z 55, 81 and 95.

CHAPTER IV CONCLUSIONS

In summary, LC/ES-MS and LC/ES-MS/MS have been shown to be useful tools for the characterization of brevetoxin metabolites. Negative mode electrospray mass spectrometry was applied to brevetoxin metabolism studies for the first time, and successfully elucidated the structure of one metabolite of brevetoxin-2. In this study, brevetoxin-2 was shown to undergo *in vitro* metabolism by rat liver microsomes to yield two metabolites. One is assigned as the hydrolysis product of the head portion six-membered lactone ring of the substrate; the other is proposed to be brevetoxin-3, the metabolically reduced product of brevetoxin-2. The experimental results shows that negative mode electrospray mass spectrometry has fewer interferences than regular positive mode electrospray mass spectrometry, and also provide a novel viewpoint to elucidate the structure of an unknown compound. However, due to the specific requirement of negative mode mass electrospray that the analytes be able to undergo deprotonation fairly easily to yield signals, the varieties of compounds that are applicable to such analysis are limited compared to that for positive mode electrospray mass spectrometry.

Brevetoxin-1 was shown to be metabolized by rat liver hepatocytes, also producing two metabolites. One is formed by transforming a double bond on the E or F ring into a diol, while the other is postulated to be a hydrolysis product of brevetoxin-1 involving opening of the head group five-membered lactone ring.

Future directions should include the development of ancillary approaches, such as anion attachment, to enhance the signal intensity of compounds that conventionally do not yield strong signal in negative mode mass spectrometry. This will broaden the applications of negative mode ES-MS to other brevetoxins and their metabolites.

REFERENCE

(1) Risk, M.; Lin, Y. Y.; MacFarlane, R. D.; Ramanujam, V. M. S.; Smith, L. L.; Trieff, N. M. **1979**; Elsevier North Holland, Inc.; 335-344.

(2) Margalef, R.; Estrada, M.; Blasco, D. In *Toxic Dinoflagellate Bloom*; Taylor, D. L., Seliger, H. H., Eds.; Elsevier: North Holland, **1979**, pp 89-94.

(3) Derby, M. L. G., Michael; Martin, Dean F.; Krzanowski, Joseph J. , Chicago, IL, USA 2001; American Chemical Society; 243-248.

(4) Baden, D. G. *FASEB J.* **1989,** *3*, 1807-1817.

(5) Pierce, R. H.; Henry, M. S.; Proffitt, L. S.; Hasbrouck, P. A. In *Toxic Marine Phytoplankton*; Granéli, E., Sundström, B., Edler, L., Anderson, D., Eds.; Elsevier Publishing Co.: New York, **1990**, pp 397-402.

(6) Steidinger, K. A. *Prog. Phycol. Res.* **1983,** *2*, 147-188.

(7) Pierce, R. H. *Toxicon* **1986,** *24*, 955-965.

(8) Dickey, R. J., Edward; Granade, Ray; Mowdy, Don; Moncreiff,Cynthia; Rebarchik, Dwan; Robl, Martin; Musser, Steven; Poli, Mark *Natural Toxins* **1999,** *7*, 157-165.

(9) Trainer, V. L. B., Daniel G. *Aquatic Toxicology* **1999,** *46*, 139-148.

(10) Lin, Y. Y.; Risk, M.; Ray, S. M.; Van Engen, D.; Clardy, J.; Golik, J.; James, J. C.; Nakanishi, K. *J. Am. Chem. Soc.* **1981,** *103*, 6773-6775.

(11) Rakotoniaina, C. A. M., D. M. *Assays for Ciguatera-Type Toxins. In: Ciguatera Seafood Toxins*; CRC Press: Boca Raton, Fl., 1991.

(12) Rein, K. S.; Lynn, B.; Gawley, R. E.; Baden, D. G. *J. Org. Chem.* **1994**, 2107-2113.

(13) Washburn, B. S.; Rein, K. S.; Baden, D. G.; Walsh, P. J.; Hinton, D. E. *Arch. Biochem. Biophy.* **1997,** *343,* 149-156.

(14) Whitney, P.; Baden, D. G. *Natural Toxin* **1996,** *4,* 261-270.

(15) Poli, M. *J. Assoc. Off. Anal. Chem* **1988,** *71,* 1000-1002.

(16) Poli, M. A. M., Steven M.; Dickey, Robert W.; Wilers, Paul P.; Hall Sherwood. *Toxicon* **2000,** *38,* 981-993.

(17) Ishida, H.; Nozawa, A.; Totoribe, K.; Muramatsu, N.; Nukaya, H.; Tsuji, K.; Yamaguchi, K.; Yasumoto, T.; Kaspar, H.; Berkett, N.; Kosuge, T. *Tetrahedron Letters* **1995,** *36,* 725-728.

(18) Murata, K.; Satake, M.; Naoki, H.; Kaspar, H. F.; Yasumoto, T. *Tetrahedron Letters* **1998,** *54,* 735-742.

(19) Morohashi, A.; Satake, M.; Murata, K.; Naoki, H.; Kaspar, H. F.; Yasumoto, T. *Tetrahedron Letters* **1995,** *36,* 8995-8998.

(20) Poli, M. A.; Templeton, C. B.; Pace, J. G.; Hines, G. B. **1990**; American Chemical Society; 176-191.

(21) Lin, J. H.; Lu, A. Y. *Pharmacological Reviews* **1997,** *49,* 403-449.

(22) Powis, G. *Drug Metabolism Reviews* **1989,** *20,* 379-394.

(23) Penman, B. W.; Reece, J.; Smith, T.; Yang, C. S.; Gelboin, H. V.; Gonzalez, F. J.; Crespi, C. L. *Pharmocogenetics* **1993,** *3,* 28-39.

(24) Li, A. P. *Drug Discovery Today* **2001,** *6,* 357-366.

(25) Yan, Z.; Caldwell, G. W. *Curent Topics in Medicinal Chemistry* **2001,** *1,* 403-425.

(26) Degawa, M.; Kanazawa, C.; Hashimoto, Y. *Carcinogensis* **1982,** *3,* 1113-7.

(27) Zhang, Q.; Ma, P.; Iszard, M.; Cole, R. B.; Wang, W.; Wang, G. *Drug Metabolism and Disposition* **2002,** *30*, 1077-1086.

(28) Ekwall, B.; Acosta, D. *Drug and Chemical Toxicology* **1982,** *5*, 219-231.

(29) Pierce, R. H.; Henry, M. S.; Proffitt, L. S.; deRosset, A. J. *Bull. Environ. Contam. Toxicol.* **1992,** *49*, 479-484.

(30) Hua, Y.; Cole, R. B. *Anal. Chem* **2000,** *72(2)*, 376-383.

(31) Hua, Y.; Lu, W.; Henry, M. S.; Pierce, R. H.; Cole, R. B. *Anal. Chem* **1995,** *67*, 1815-1823.

(32) Kawada, M. T., Hisashi; Kagawa, Yasuo; Szuki, Kantaro; Shimazono, Norio *J. Biochem. (Tokyo)* **1962,** *51*, 405-15.

(33) Sun, G.; Alexson, S. E. H.; Harrison, E. H. *Journal of Biological Chemistry* **1997,** *272*, 24488-24493.

(34) Williams, F. M.; Mutch, E.; Blain, P. G. *Biochemical Pharmacology* **1991,** *41*, 527-531.

VITA

Weiqun Wang was born on June 13, 1968 in Tianjin, People's Republic of China. He graduated from Nankai University in 1989 and obtained his B.S. degree in Chemistry. He then worked as an assistant engineer at Tianjin Automobile Company to 1991. Later he obtained his M.S. in Chemistry in 1994 from Nankai University and worked at Second Hospital of Tianjin Medical University until he came to University of New Orleans in 1999 to pursue his PhD. degree.